Paper ID
AEC1027

The 3d TSME International Conference on Mechanical Engineering
October 2012, Chiang Rai

Measures for Reliable and Effective Operation of a Conical Fluidized-Bed Combustor Fired with Oil Palm Shells: A Combustion Study

Pichet Ninduangdee and Vladimir I. Kuprianov*

School of Manufacturing Systems and Mechanical Engineering, Sirindhorn International Institute of Technology, Thammasat University, Pathum Thani 12121, Thailand
*Corresponding Author: E-mail address: ivlaanov@siit.tu.ac.th; tel.: +66 2 986 9009, ext. 2208; fax: +66 2 986 9112

Abstract

The fluidized-bed combustion of high-alkali biomass fuels is associated with a high risk of bed agglomeration. To avoid this ash-related problem, oil palm shells (with elevated potassium content in fuel ash) were burned in the conical fluidized-bed combustor (FBC) using alumina sand as the bed material. In this combustor, the fluidized bed was generated and sustained by a newly proposed 19-bubble-cap air distributor. Combustion tests were performed at two fuel feed rates, 45 kg/h and 30 kg/h, when ranging excess air from about 20% to 100% for each combustor load. In order to characterize combustion and emission performance of the conical FBC, temperature and gas concentrations (O_2, CO, C_xH_y as CH_4, and NO) were recorded along radial and axial directions in the reactor as well as at stack. For the ranges of operating conditions, the combustion efficiency was found to be high, 98.0–98.4%, while the major gaseous emissions of the combustor (CO and NO) were ensured at acceptable levels meeting the national emission limits. Neither bed agglomeration nor significant ash deposit on the combustor walls were observed during the entire test period of about 30 h. However, the chemical composition of the bed material and that of fly ash originated from the combustion exhibited substantial time-domain changes during the combustion of oil palm shells.

Keywords*:* Oil palm shells; Fluidized-bed combustion; Emissions; Combustion efficiency; Ash behavior

1. Introduction

Palm oil industry is one of the major sectors in the Thai economy. During oil palm processing, a significant amount of solid residues, such as empty fruit bunches, oil palm fiber and shells, palm fronds and leaves, are produced in Thailand, which is equivalent to the energy potential of ~3000 ktoe/year [1]. Most of the oil palm mills are equipped with a small-scale power plant fired with some of these biomass residues to generate heat and power for oil production [2].

The fluidized-bed combustion technology is proven to be one of the most effective and environmental friendly technologies for energy conversion from biomass residues [3,4]. However, the combustion of high-alkali biomass fuels (particularly, oil palm residues) in a fluidized bed using silica sand as the fluidizing agent (also termed ‘bed material’) is often accompanied by operational problems, such as bed accumulation and agglomeration [3,5–7]. A continuous formation of agglomerates (basically composed of the bed material particles with affiliated mass of ash) in the fluidized bed, occurring even at a relatively low combustion temperature (750–800 °C), becomes a cause of bed defluidization, leading to immediate shutdown of the combustion system [3].

In order to prevent bed agglomeration, some alternative bed materials, such as alumina, dolomite, pre-calcined bauxite, ferric oxide and commercial bed material (GR Granule), which can be potentially employed in fluidized-bed combustion systems, have been discussed in a number of research studies [8–12]. These bed materials with some important metals, such as aluminum, magnesium, calcium and iron, prevent bed agglomeration, mainly due to formation of eutectics with high (or very high) fusion temperature, which are generally formed in chemical reactions between alkali compounds vaporized from biomass ash and the bed material.

A conical fluidized-bed combustor (‘conical FBC’) using a relatively small amount of the bed material [4] seems to be the most suitable fluidized-bed combustion technique for testing the alternative (typically, high-cost) bed materials.

The main objective of this study was to investigate a feasibility of reliable and effective burning of oil palm shells in the conical FBC using alumina as the fluidizing agent for the range of operating conditions (fuel feed rate and excess air). Combustion and emission performance of the combustor, as well as the capability of the bed material to withstand bed agglomeration were the focus of this experimental study.

2. Methodology

2.1 Experimental set-up

Fig. 1 shows the experimental set up, including the conical FBC and auxiliary equipment, as well as the design and geometrical details of the combustor (reactor).

The combustor was designed to operate with up to 250 kW_{th} heat input when burning oil palm shells. It consisted of two steel sections assembled coaxially: (1) a conical section of 0.9 m height with the cone angle 40° and 0.25 m outer diameter at the bottom plane, and (2) a cylindrical section comprising five cylindrical modules of 0.5 m height and 0.9 m inner diameter. Both sections had 4.5-mm thick metal walls lined internally with the refractory-cement insulation of 50 mm thick. To measure gas concentrations and temperature in combustion products (flue gas), the combustor was equipped with gas sampling ports and stationary Chromel-Alumel thermocouples (of type K) located at different levels along the combustor height, as well as at the cyclone exit

Besides the combustor, the experimental set up included (i) a start-up burner fixed at a level of 0.5 m above the air distributor and titled at an angle of –30° angle with respect to the horizon (for preheating sand prior to the combustor operation), (ii) a screw-type fuel feeder arranged at a level of 0.6 m above the air distributor (for feeding biomass to the reactor), (iii) a 25-hp blower (to supply combustion air), (iv) a cyclone arranged downstream from the combustor (to collect particulates from the stack gas), as well as (v) some facilities for data acquisition and treatment.

The air blower delivered air to the combustor through an air pipe of 0.1 m inner diameter. Air was injected into the sand bed through the modified air distributor with nineteen bubble caps arranged at a bottom plane of the conical module. The air distributor generated and sustained the fluidized bed in the conical section providing a uniform distribution of airflow over the bed at a quite low pressure drop across the device.

2.2 The fuel and the bed material

The preliminary (set up) combustion tests of the conical FBC for firing oil palm shells with original (coarse) particles showed a serious problem in stable fuel feeding when using the above-mentioned screw feeder. To ensure smooth feeding of fuel to the combustor and also to improve hydrodynamic characteristics of the fluidized bed, oil palm shells were shredded prior to experimental tests using a shredder driven by a 7.5-hp electric motor. However, shape and size of shredded oil palm shells were quite irregular: from fine sawdust-like particles to flake-shape particles with the maximum sieved particle size of about 12 mm.

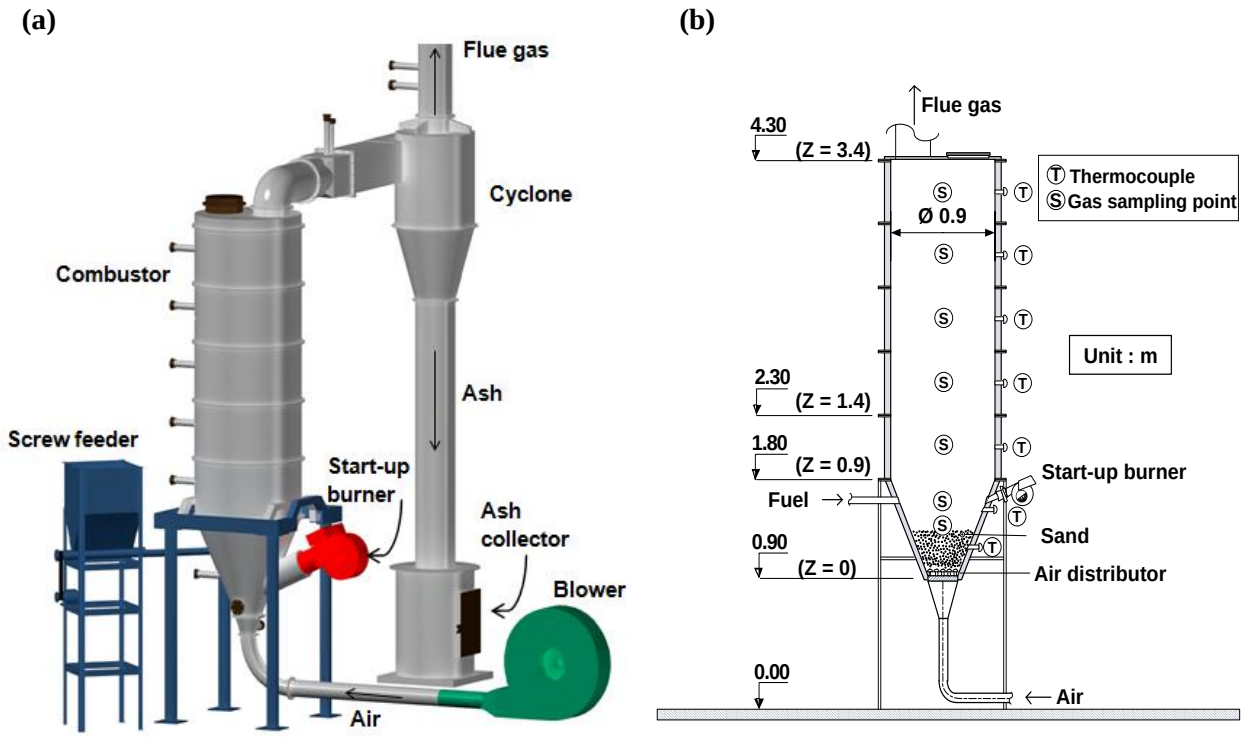

Fig. 1 (a) Experimental set up with the conical FBC and (b) geometrical characteristics of the combustor

Table 1 Ultimate and proximate analyses and lower heating value (LHV) of oil palm shells

Ultimate analysis (wt.%, as-received basis)						Proximate analysis (wt.%, as-received basis)				
C	H	O	N	S		W	A	VM	FC	LHV (kJ/kg)
48.06	6.98	38.69	1.27	0.09		5.4	4.7	71.7	18.8	16,300

Table 1 shows the ultimate and proximate analyses, as well as the lower heating value (LHV) of oil palm shells used in this study on the conical FBC. As seen in Table 1, the proximate analysis of oil palm shells included a significant amount of volatile matter, whereas moisture and ash contents in the fuel were at quite low levels, which resulted in the substantial heating value of oil palm shells: LHV = 16,300 kJ/kg. Because of the extremely low content of sulfur (less than 0.1%), SO_2 was not addressed in this study.

Alumina sand with a solid density of about 3500 kg/m^3 and particle size 0.3–0.5 mm was used as the bed material in this combustor with the aim to prevent bed agglomeration during the combustion tests. In all test runs, the static bed height of alumina sand was fixed at 30 cm.

Table 2 shows the chemical composition of alumina sand, which was obtained using an X-ray fluorescent spectroscopy – the Philips PW2400 XRF spectrometer. As seen in Table 2, Al_2O_3 was the predominant component in this bed material.

2.3 Experimental procedure

A diesel start-up burner of the Riello Burners Company (model "Press G24") was used to preheat the bed material during the combustion start up. When the bed temperature reached about 700 °C, a diesel pump of the burner was turned off. However, during the combustion tests, a burner fan continued its operation with a minimum airflow rate to protect a nozzle head of the burner from overheating. In the meantime, a rectangular 20 cm × 30 cm steel curtain was used to screen the burner from the combustion chamber and thus to avoid impacts by flame and particulates when the burner was out of service.

The screw-type feeder delivered shredded oil palm shells into the conical module at a level Z = 0.6 m above the air distributor, as shown in Fig. 1b. A three-phase inverter was used to control the fuel feed rate via adjusting the rotational speed of the screw feeder. The experimental tests were performed for two values of the fuel feed rate (FR): 45 kg/h and 30 kg/h.

To investigate the combustion and emission characteristics in different regions of the reactor, a model Testo-350XL gas analyzer was used to measure temperature and gas concentrations (O_2, CO, C_xH_y and NO) along radial and axial directions inside the combustor, as well as at the cyclone exit. The measurement accuracies were ±0.5% for temperature, ±5% for CO within the range of 100–2000 ppm, ±10% for CO higher than 2000 ppm, ±10% for C_xH_y up to 40,000 ppm (as CH_4), ±5% for NO, and ±0.2 vol % for O_2.

Excess air (EA) was estimated using the excess air ratio determined using experimentally found O_2, CO and C_xH_y (as CH_4) in "dry" flue gas at the cyclone exit [13]. Note that the experiments for the emission performance and combustion efficiency were performed at each combustor load for five specified values of excess air: 20%, 40%, 60%, 80% and 100%. However, the detail investigation of formation/decomposition of major pollutants was performed for only two values of excess air: 40% and 80%.

The heat-loss method was employed to determine the combustion efficiency for various operating conditions [13]. To quantify the heat loss due to unburned carbon, fly ash was analyzed for carbon content. However, the heat loss due to incomplete combustion was predicted according to Ref. [13] based on the CO and C_xH_y (as CH_4) emissions and using relevant combustion parameters (excess air, fuel lower heating value and volume of "dry" combustion products at stack).

After the combustor testing during 10, 20 and 30 h, the bed material and also fly ash were sampled and analyzed for their chemical composition using a wavelength dispersive X-ray fluorescence spectrometer to determine time-sale effects on the chemical composition of both the bed material and fly ash. A scanning electron microscopy (SEM) technique was used to determine a physical texture of the bed particles after different operating time periods.

Table 2 Chemical composition of alumina sand (wt.%) prior to the combustion study on the conical FBC

Al_2O_3	SiO_2	Fe_2O_3	CaO	MgO	Na_2O	ZnO	P_2O_5
99.40	0.09	0.07	0.05	0.03	0.38	0.03	0.01
±2.59	±0.07	±0.02	0.02	0.03	0.09	-	-

3. Results and Discussion

3.1 Radial and axial temperature and gas concentration profiles in the conical FBC

Fig. 2 depicts the radial temperature and gas concentration profiles in the conical FBC firing 45 kg/h oil palm shells at excess air of about 40% at three different levels (Z) above the air distributor. It can be seen in Fig. 2 that the radial temperature profiles were quite uniform at all the levels inside the reactor, thus, indicating intensive heat-and-mass transfer along the radial direction. In the meantime, the radial O_2, CO, C_xH_y and NO concentration profiles were rather/fairly uniform which can be explained by intensive gas–solid and gas–gas mixing in the radial direction as well as by uniform distribution of air across the bed. Due to uniformity of the radial profiles, the axial temperature and concentration profiles were therefore used to characterize combustion and emission performance of the conical FBC.

Fig. 3 depicts the axial temperature and O_2 concentration profiles in the combustor firing oil palm shells at the specified fuel feed rates (45 kg/h and 30 kg/h) for excess air values of about 40% and 80%. It appears that in the conical section of the reactor, the axial temperature profiles had a slight positive gradient along the combustor height (mainly due to the endothermic drying and devolatilization of fuel particles), whereas in the cylindrical section these profiles exhibited a reducing trend of temperature along the combustor height (apparently caused by heat losses across the reactor walls). The reduction in the combustor load (i.e., fuel feed rate) led to a decrease in temperature at any point inside the combustor because of lower heat input to the combustor. Meanwhile, a local temperature drop was observed when increasing excess air, which

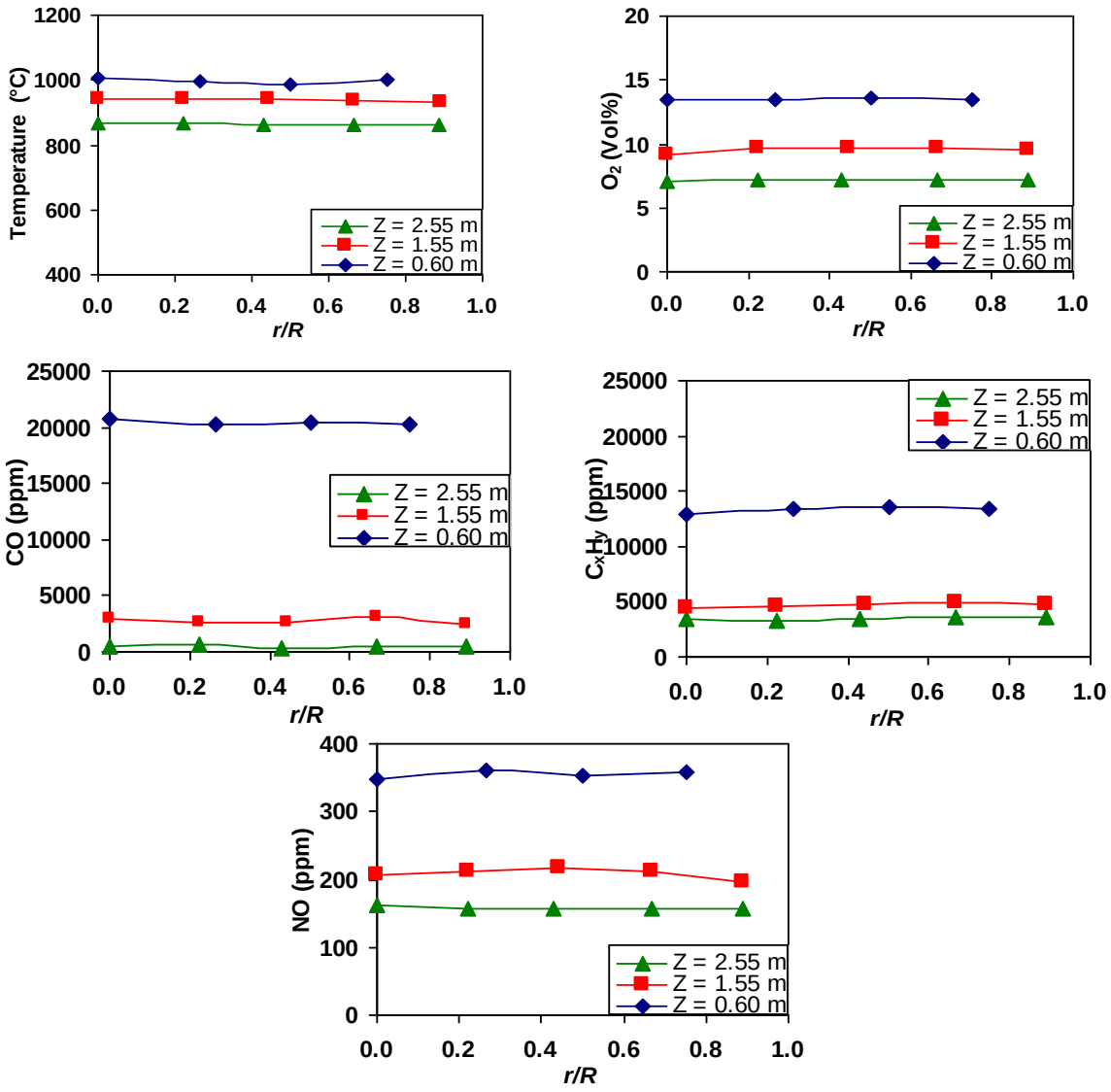

Fig. 2 Radial temperature and O_2, CO, C_xH_y and NO concentration profiles at three levels (Z) in the conical FBC when firing 45 kg/h oil palm shells at excess air of about 40%

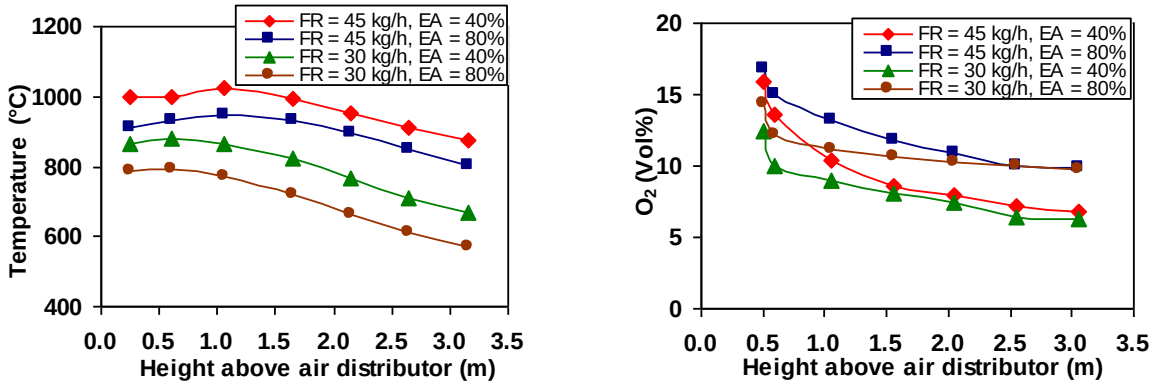

Fig. 3 Effects of operating conditions – fuel feed rate (FR) and excess air (EA) – on the axial temperature and O_2 concentration profiles in the conical FBC when firing oil palm shells

can be explained by apparent air dilution effects.

In all the test runs, the axial O_2 concentration profiles exhibited a gradual diminishing along the combustor height. However, the behavior of O_2 indicates that a significant proportion of fuel was oxidized in the bottom region of the combustor, as can be seen in Fig. 3. At the reduced combustor load, the rate of O_2 consumption in this region was somewhat higher (despite the reduction in the bed temperature) compared to that maximum load for similar excess air, which can be explained by a increase in the residence time of the reactants. In the meantime, with increasing excess air at fixed combustor load, the O_2 concentration was somewhat higher at all points inside the reactor.

Fig. 4 compares the axial CO, C_xH_y (as CH_4) and NO concentration profiles in the conical FBC between the two fuel feed rates and excess air values. All the profiles revealed two specific regions in the reactor – the bottom region ($0 < Z < 0.6$ m) and the upper region ($Z > 0.6$ m) – within which a net result of formation/decomposition of the gaseous pollutants was quite opposite.

In the bottom region, a significant rise of CO was observed for the two combustor loads, mainly, due to the rapid fuel devolatilization and, also, oxidation of C_xH_y and char-C to CO. For selected excess air, the peak of CO concentration

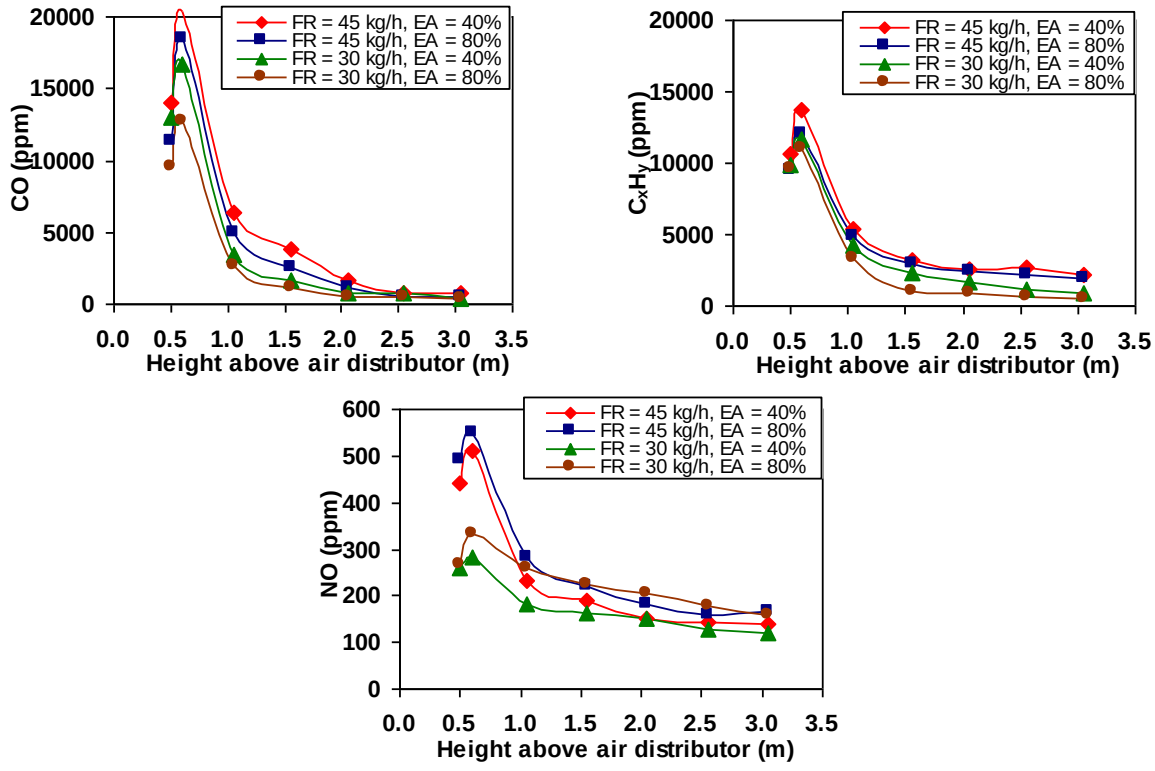

Fig. 4 Effects of operating conditions – fuel feed rate (FR) and excess air (EA) – on the axial CO, C_xH_y (as CH_4) and NO concentration profiles in the conical FBC when firing oil palm shells

at the reduced load was somewhat lower compared to that at the maximum fuel feed rate, primarily, due to the increased residence time (which caused a higher contribution of CO decomposition in this region). In the upper region, the CO concentration was gradually reduced (with the reduction rate being weakly dependent on the fuel feed rate), mainly due to oxidation of CO by O_2 (from excessive air) and OH [14]. It should be noted that an increase excess air (at fixed combustor load) led to the lowering of the CO peak (observed at $Z \approx 0.6$ m), mainly due to the enhanced rate of CO oxidation by O_2.

The axial C_xH_y concentration profiles had similar trends as those for CO at different fuel feed rates and excess air levels and exhibited similar effects of the operating conditions. As well known, C_xH_y are basically originated from fuel volatile matter and oxidized forming CO as an intermediate product [14]. Since CO received the continuous "feeding" from oxidation of C_xH_y and char-C, the concentration of CO at different locations in the combustor were substantially higher than that of C_xH_y for the ranges of operating conditions.

From the graph with the axial NO concentration profiles (see Fig. 4), in the first region, NO was found to be rapidly increased in all the test runs. As known, NO is formed from volatile nitrogenous species (mainly, NH_3), through the fuel-NO formation mechanism including the proportional effects of fuel N, temperature and excess air. Simultaneously, a part of NO is decomposed due to catalytic reduction of NO by CO on a surface of char, ash and bed material particles [3,14]. Thus, within the first region, the rate of NO formation was significantly greater than that of NO decomposition. However, in the upper region, a significant drop of NO was observed, mainly due to the NO decomposition reactions, while the rate of NO formation was negligible. At a level *Z*, where formation and decomposition rates were equal, the axial NO concentration profiles exhibited a maximum, which was dependent on operating conditions. For the reduced combustor load, the NO peaks were substantially lower because of the lower bed temperature and greater residence time, which likely resulted in a greater contribution of NO decomposition in the bottom part of the reactor, whereas in the upper region the effects of load were quite complicated. In the meantime, with reducing excess air at fixed load, NO at all locations along the combustor height was somewhat lower (in accordance with the above-mentioned fuel-NO formation mechanism).

3.2 Emissions and combustion efficiency

Table 3 summarizes the major gaseous emissions (presented on a dry gas basis and at 6% O_2), as well as the heat losses (due to unburned carbon and incomplete combustion) and the combustion efficiency of the conical FBC when firing oil palm shells at specified fuel feed rates and excess air values.

It can be seen in Table 3 that with reducing the combustor load, all the emissions showed the diminishing trend (at any arbitrary excess air value), which can be explained by an increase in the residence time (for CO and C_xH_y emissions) as well as by the reduced combustion temperature

Table 3 Emissions and combustion efficiency of the conical FBC when firing with oil palm shells for variable operating conditions

Excess air (%)	Emission [a]			Heat loss (%):		Combustion efficiency (%)
	CO	C_xH_y	NO	due to unburned carbon	due to incomplete combustion	
Fuel feed rate = 45 kg/h						
18	739	2238	81	0.73	2.60	96.7
40	299	1168	143	0.30	1.87	97.8
59	203	864	176	0.27	1.77	98.0
79	163	600	204	0.22	1.68	98.1
99	142	453	236	0.11	1.50	98.4
Fuel feed rate = 30 kg/h						
22	448	1360	68	0.46	1.61	97.9
40	85	740	122	0.22	0.96	98.8
58	24	460	178	0.19	1.06	98.8
78	25	230	200	0.17	0.47	99.4
99	40	162	213	0.09	0.52	99.4

[a] At 6% O_2 (on a dry gas basis).

(important for NO formation).

At the maximum combustor load and lowest excess air (about 20%), the CO and C_xH_y emissions from the combustor were at highest levels: 739 ppm and 2238 ppm, respectively. However, with increasing excess air, both CO and C_xH_y emissions were substantially decreased. Thus, these emissions can be effectively controlled via maintaining excess air at an appropriate level.

Unlike CO and C_xH_y, the emission of NO showed quite opposite effects of excess air. With increasing excess air, the NO emission from the combustor was higher, thus confirming the fuel-NO formation mechanism and pointing at a substantial contribution of CO and C_xH_y to the NO decomposition (especially, at low excess air).

As seen in Table 3, the combustion efficiency for both fuel feed rates exhibited an apparent improvement when increasing excess air. At excess air values of 40–100%, the combustion efficiency was nearly the same and characterized by a highest value for each combustor load. Thus, at the 45 kg/h fuel feeding, the combustion efficiency of 97.8–98.4% can be achieved if the combustor is operated at excess air of 40–100%. At the reduced combustor load, the combustion efficiency becomes somewhat higher, by 0.5–1.0%, at apparently lower combustor emissions.

Taking into consideration the emission characteristics as well as combustion efficiencies in Table 3, excess air of about 60% seems to be an optimal value for firing oil palm shells in the conical FBC using alumina sand as the bed material. For the maximum combustor load and optimal excess air, the combustor can be operated with high combustion efficiency, ~98.0%, and the major emissions can be controlled at acceptable levels: 203 ppm for CO and 176 ppm for NO (both meeting corresponding domestic emission limits for the biomass-fuelled industrial applications [15]), while maintaining C_xH_y at a reasonable level and also avoiding very high bed temperatures occurred at excess air of 20–40%.

3.3 Timescale effects on physical properties of the bed material

By visual inspections after each 10 h of combustor operation, no significant changes in size and shape of the bed material particles were found compared to the particles of original alumina sand. Besides, neither bed agglomeration nor significant ash deposit on the combustor walls were observed during the entire test period (about 30 h). After all experiments, the bed material exhibited normal appearance (grains) capable to fluidize and thus be used in further studies.

Fig. 5 illustrates the SEM images of original alumina sand and that of the bed material after all the experiments. It can be seen in Fig. 5 that the external surface of original alumina exhibited some roughness. Furthermore, as can be seen in the image obtained with higher magnification, the internal texture of alumina can be basically characterized as porous. From the SEM images of the bed particles after 30-h combustor operation, the external surface of the bed particles showed an apparent increase in its roughness indicating the formation of a coating layer on the bed particle surface. From the higher magnification, the internal surface of the bed particles (i.e.,

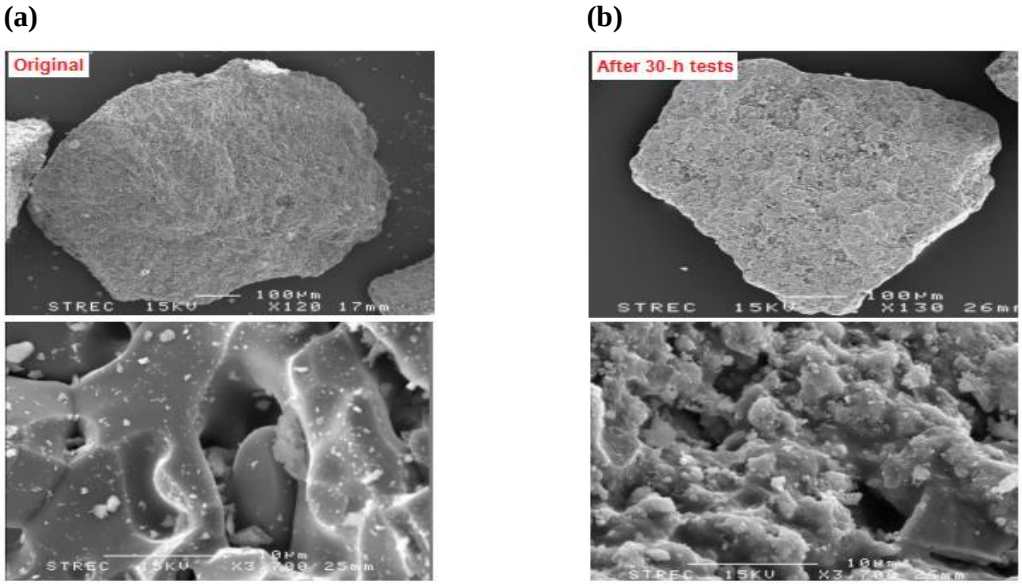

Fig. 5 SEM images of (a) original alumina sand and (b) bed material particles after 30-h tests, both represented with different magnifications: ×120 (or ×130) and ×3700

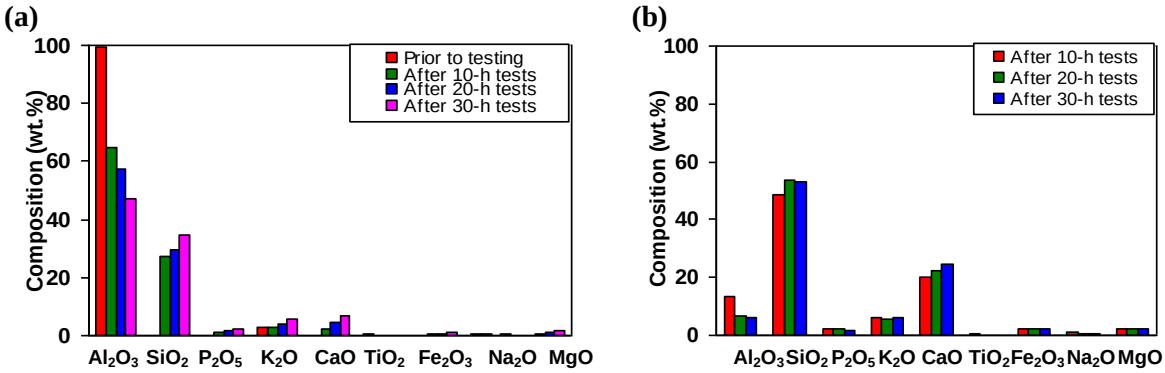

Fig. 6 Time-scale effects on the composition of (a) the bed material and (b) fly ash originated from the combustion of oil palm shells (all oxides are given at different time instants of combustor operation)

surface of minute interstices) was covered by a quite thin layer composed of solidified compounds, likely originated from reactions of vaporized alkali salts of ash with the bed particle on its external and internal surfaces.

3.4 Timescale effects on chemical properties of the bed material and fly ash

Fig. 6 shows the composition of original alumina sand and that of the used bed material (as oxides in both analyses) after different time periods (10, 20 and 30 h) of combustor operation. As revealed by data in Fig. 6a, the content of SiO_2, CaO and K_2O in the bed material increased with time, whereas Al_2O_3 showed a substantial reduction, by about 50%, after 30-h combustor operation. Thus, the bed material diminishes its capability to withstand the bed agglomeration with time. From Fig. 6b, Al_2O_3 in the fly ash after first 10-h operation was higher compared to other samples, which indicated an intensive loss of the original bed material at the initial stage of the combustor operation.

As can be concluded from analysis of the time-domain behavior of the bed material and fly ashes (exhibited by their chemical compositions), a sensible bed accumulation might occur along with the burning of oil palm shells in the conical FBC. However, a physical mass of the bed material increased by an insignificant value (about 5%) during the entire operational time period. Furthermore, no sensible change occurred with particle size of the bed material during the tests, as confirmed by visual observations of the fluidizing agent. Such a result can be explained by the collisions, breakage and attrition of the bed material particles, apparently causing destruction of the coating, followed by its carryover from the combustor. Analysis of ash composition (an appearance of elevated Al_2O_3 in fly ashes) confirms this conclusion.

4. Conclusions

The conical fluidized-bed combustor has been successfully tested for burning shredded oil palm shells at fuel feed rates of 45 kg/h and 30 kg/h, while ranging excess air from 20% to 100%. This study revealed that reliable and effective operation of the combustor is achievable when using alumina sand as the bed material.

The specific conclusions derived from this study are as follow:

- the radial temperature and gas (O_2, CO, C_xH_y as CH_4, and NO) concentration profiles at different levels inside the combustor are rather (or fairly) uniform. This fact allows analyzing the combustion and emission performance of the conical FBC using the axial profiles of this variables;
- the major operating conditions (fuel feed rate and excess air) affect sensibly the combustion and emission characteristics of the combustor;
- at 45 kg/h fuel feeding, high (97.8–98.4%), combustion efficiency of the conical FBC is achievable when burning oil palm shells at excess air of 40–100%. However, the best emission performance – acceptable levels of CO and NO emissions (i.e., meeting the national emission limits) and a reasonable level of C_xH_y emissions – can be ensured when applying 60% excess air;
- no evidence of bed agglomeration was found during 30-h experimental tests on this conical FBC using alumina sand as the bed material. However, as reveal by SEM images, the bed material surfaces showed an increase in the roughness of the bed particles, indicating the formation of a coating layer on the surface of these particles;
- the composition of bed material and fly ash undergoes substantial changes during combustor operation, indicating a gradual loss of the bed capability to withstand bed agglomeration.

5. Acknowledgement

The authors wish to acknowledge the financial support from the Bangchak Petroleum Public Company Limited.

6. References

[1] DEDE (2010). Annual report on Thailand Alternative Energy Situation. The Department of Alternative Energy Development and Efficiency, Ministry of Energy, Thailand.

[2] Prasertsan, S. and Prasertsan, P. (1996). Biomass residues from palm oil mills in Thailand: an overview on quantity and potential usage. *Biomass and Bioenergy*, vol. 11, pp. 387–395.

[3] Werther, J., Saenger, M., Hartge, E.-U., Ogada, T. and Siagi, Z. (2000). Combustion of agricultural residues, *Progress in Energy and Combustion Science*, vol. 26, pp. 1–27.

[4] Permchart, W. and Kouprianov, V.I. (2004). Emission performance and combustion efficiency of a conical fluidized-bed combustor firing various biomass fuels, *Bioresource Technology*, vol. 92, pp. 83–91.

[5] Saenger, M., Hartge, E.-U., Werther, J., Ogada, T. and Siagi, Z. (2001). Combustion of coffee husks, *Renewable Energy*, vol. 23, pp. 103–121.

[6] Chaivatamaset, P., Sricharoon, S., and Tia, S. (2011). Bed agglomeration characteristics of palm shell and corncob combustion in fluidized bed, *Applied Thermal Engineering*, vol. 31, pp. 2916–2927.

[7] Ohman, M. and Nordin, A., (2000). Bed Agglomeration Characteristics during Fluidized Bed Combustion of Biomass Fuels, *Energy & Fuels*, vol. 14, pp. 169–178.

[8] Shimizu, T., Han, J., Choi, S., Kim, L. and Kim, H. (2006). Fluidized-Bed Combustion Characteristics of Cedar Pellets by Using an Alternative Bed Material, *Energy & Fuels*, vol. 20, pp. 2737–2742.

[9] Sun, Z., Jin, B., Zhang, M., Liu, R. and Zhang, Y. (2008). Experimental studies on cotton stalk combustion in a fluidized bed, *Energy*, vol. 33, pp. 1224–1232.

[10] Arromdee P. and Kuprianov, V. I. (2012). Combustion of peanut shells in a cone-shaped bubbling fluidized-bed combustor using alumina as the bed material. *Applied Energy*, vol. 97, pp. 470–482.

11] Llorente, M. J. F., Arocas. P.D, Nebot, L. G. and Carcia, J. E. C. (2008). The effect of the addition of chemical materials on the sintering of biomass ash, *Fuel*, vol. 87, pp. 2651–2658.

[12] Bartels, M., Lin, W., Nijenhuis, J., Kapteijn, F. and Ommen, J. R.V., 2008. Agglomeration in fluidized beds at high temperatures: Mechanisms, detection and prevention. *Progress in Energy and Combustion Science*, 34, pp. 633–666.

[13] Basu, P., Cen, K.F. and Jestin, L. (2000). Boilers and Burners, Springer, New York.

[14] Turns, S. (2006). An Introduction to Combustion, McGraw-Hill: Boston.

[15] Pollution Control Department, Ministry of Natural Resources and Environment, Thailand. Air pollution standards for industrial sources. http://www.pcd.go.th/info_serv/reg_std_airsnd03.html.